RUSSIAN JOURNAL OF EARTH SCIENCES, VOL. 9, ES2002, doi:10.2205/2007ES000297, 2007

Two spinel populations from the Cretaceous-Paleogene (K/T) boundary clay layer in the Gams stratigraphic sequence, Eastern Alps

A. F. Grachev[1], V. A. Tselmovich[2], O. A. Korchagin[3], and H. A. Kollmann[4]

Received 21 September 2007; accepted 9 November 2007; published 20 November 2007.

[1] The K/T boundary layer in the Gams stratigraphic sequence, Eastern Alps, was determined to contain two spinel populations. One of them is dominated by Cr spinel, which originated from eroded high-pressure metamorphic rocks of eclogite composition, which are widespread in the Eastern Alps. This spinel is not only typical of the whole K/T boundary layer but was also found farther upsection in Maestrichtian clay. The other spinel population principally differs from the first one in having high Ni concentrations. Ni spinel from the Gams section differs by the high content of zinc (up to 5.6% in a rust crust), that is not characteristic for other known sections at the K/T boundary. Alongside with well expressed crystals octahedral forms, one grain of drop-like mode of Ni spinel has been found. It is considered, that Ni spinel is confined to 1–3 mm rust colored layer which has deposited in less than 100 years, while in the Gams section it meets in all parts of the transition layer. The question of origin Ni spinel from the transitional layer at the K/T boundary remains opened and demands the further researches. *INDEX TERMS:* 1051 Geochemistry: Sedimentary geochemistry; 1519 Geomagnetism and Paleomagnetism: Magnetic mineralogy and petrology; 3665 Mineralogy and Petrology: Mineral occurrences and deposits; 5420 Planetary Sciences: Solid Surface Planets: Impact phenomena, cratering; *KEYWORDS:* K/T boundary, spinel, impact, Eastern Alps.

Citation: Grachev, A. F., V. A. Tselmovich, O. A. Korchagin, and H. A. Kollmann (2007), Two spinel populations from the Cretaceous-Paleogene (K/T) boundary clay layer in the Gams stratigraphic sequence, Eastern Alps, *Russ. J. Earth. Sci., 9,* ES2002, doi:10.2205/2007ES000297.

Introduction

[2] The nature of the transitional layer at the boundary of the Cretaceous and Paleogene (K/T boundary layer), which is known to occur at all continents, except only Antarctica, and at the oceanic floor (deep sea drilling data) remains a matter of vivid discussions. The anomalies of Ir and other PGE elements detected in clays from the K/T boundary layer [*Alvarez et al.,* 1980 and others] gave rise to the paradigm that the massive extinction of the biota was related to an impact even and triggered the study of the boundary at several regions worldwide. The hypothesis was underlain by the reasonable idea that the high Ir concentrations (which are higher than those known in terrestrial rocks) were caused by the fall of a meteorite (or asteroid) [*Alvarez et al.,* 1980 and others].

[3] At the same time, data were published that an Ir anomaly may occur both below and above the K/T boundary [*Ellwood et al.,* 2003; *Graup and Spettel,* 1989; and others]. Moreover, Ir anomalies were also found in rocks showing no relations at all to the Cretaceous-Paleogene boundary [*Dolenec et al.,* 2000; *Keller and Stinnesbeck,* 2000; and others].

[4] Our detailed biostratigraphic, lithological, isotopic-geochemical, and magnitological examination of the stratigraphic section of the sedimentary deposits at the Cretaceous-Paleogene boundary near Gams, Eastern Alps, Austria, led us to conclude that the boundary layer was formed in two stages [*Grachev et al.,* 2005, 2006, 2007]. During the first of these stages (which lasted for approximately 1500 years at conservative assays of the sedimentation rate), the boundary layer was produced under the effect of volcanic aerosol, which predetermined the occurrence of titanomagnetite, Au, and Cu, along with high concentra-

[1]Schmidt Institute of Physics of the Earth, Russian Academy of Sciences, Moscow, Russia
[2]Geophysical Observatory, Schmidt Institute of Physics of the Earth, Russian Academy of Sciences, Borok, Yaroslavl oblast, Russia
[3]Geological Institute, Russian Academy of Sciences, Moscow, Russia
[4]Museum of Natural History, Vienna, Austria

ISSN: 1681–1208 (online)

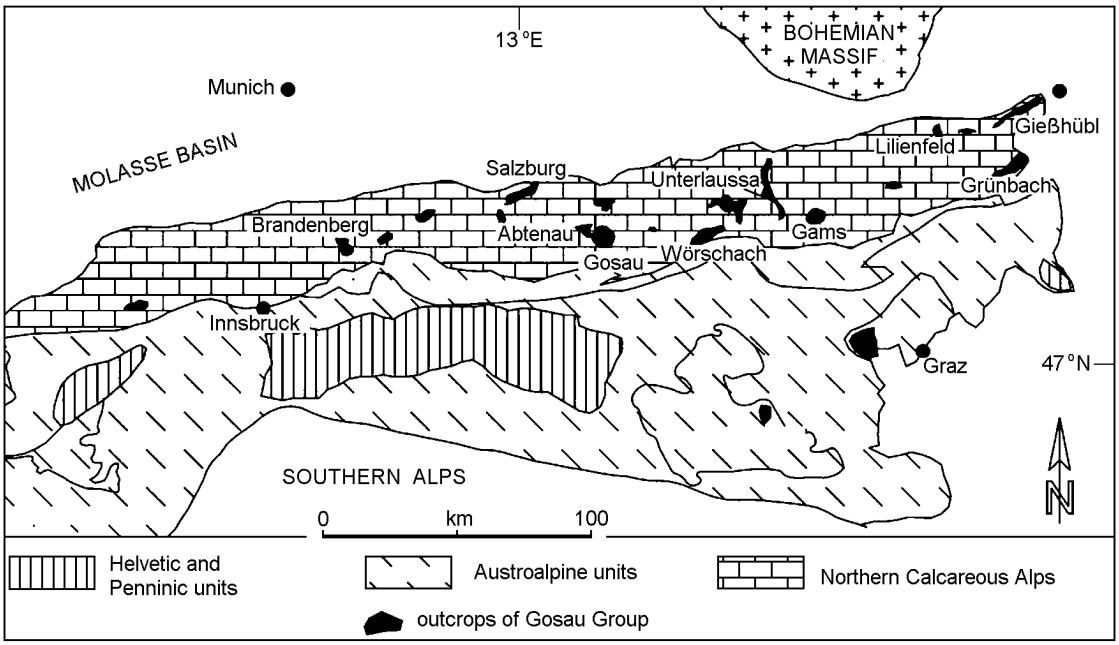

Figure 1. Localities of the Gosau Group of the Northern Calcareous Alps in the Eastern Alps [*Wagreich and Krenmayr,* 2005].

tions of Ir, As, Zn, Ni, Cr, and other element. The presence of an Ir anomaly in the lower portion of the boundary layer, as well as the occurrence of titanomagnetite, Au, and Cu in it, was related to volcanic activity. During the second stage, the character of sedimentation was affected by the fall of an asteroid (meteorite), whose traces are identified in the form of spherules of pure Ni, awaruite, and diamond crystals. Our conclusions differ from the results obtained by all other researchers dealing with the K/T boundary layer.

[5] This paper reports our newly obtained data on the composition of spinel from the Gams stratigraphic sequence not far from the village of Gams in Styria, Eastern Alps, where the Gams River exposes a number of sites with the K/T boundary layer (Figure 1).

Sampling Procedure, Sample Preparation Techniques, and Study Methods

[6] Samples from the boundary layer were first collected from a monolith cut out of an exposure and provided for us by courtesy of the administration of the Museum of Natural History in Vienna. Additional samples were then collected at exposures to ensure the reproducibility of the results.

[7] The monolith had a height of 46 cm, a width of 30 cm in its bottom portion and 22 cm at the top, and a thickness of 4 cm (Figure 2). For its comprehensive examination, the monolith was divided (vertically, from bottom to top) into layers 2 cm thick (which were labeled A, B, C, ..., W), and each of them was then subdivided into fragments by lines spaced 2 cm apart (the fragments were labeled 1, 2, 3, etc.). Layer J (2 cm thick) at the K/T boundary was examined more thoroughly and subdivided into six units approximately 3 mm each [see *Grachev et al.,* 2005 for details].

[8] In exposure Gams 2, where the thickness of the boundary layer reaches 5 cm, samples were collected in the form of continuous blocks, which were then cut into individual slices, with cutting surfaces spaced approximately 1 cm apart.

[9] Samples 10–15 g in mass were crushed in a porcelain mortar and sieved through a 0.25-mm screen. Heavy-fraction minerals were separated from the carbonate-clay mass in heavy liquids (bromoform, density 2.89 g cm^{-3}). The heavy and light fractions were washed in alcohol and purified of the magnetic fraction (magnetite) with the use of a simple magnet. The heavy-fraction minerals were separated on a magnetic separator according to their electric conductivity into a non-electromagnetic, weakly electromagnetic, and electromagnetic fractions.

[10] Other minerals were hand-picked under a binocular magnifier, using a needle and were glued to glass platelets with pits. The glue was Sherlok, which can be dissolved in alcohol. Quartz was obtained from the light fraction (<2.89 g cm^{-3}) by electromagnetic separation. In order to analyze the composition and microstructures of ferromagnetic minerals in the rocks, the samples were examined on a Camebax microprobe equipped with three wave-dispersive spectrometers and then on a Tescan Vega I and Tescan Vega II microprobes equipped with energy- and wave-dispersive spectrometers. Samples were usually mounted onto a pellet 26 mm in diameter using Wood's metal, carefully polished and finished with diamond pastes, and then sputter-coated with carbon. The analyses were conducted at an accelerating voltage of 20 kV and a beam current of 10 nA. The elements determined using their character-

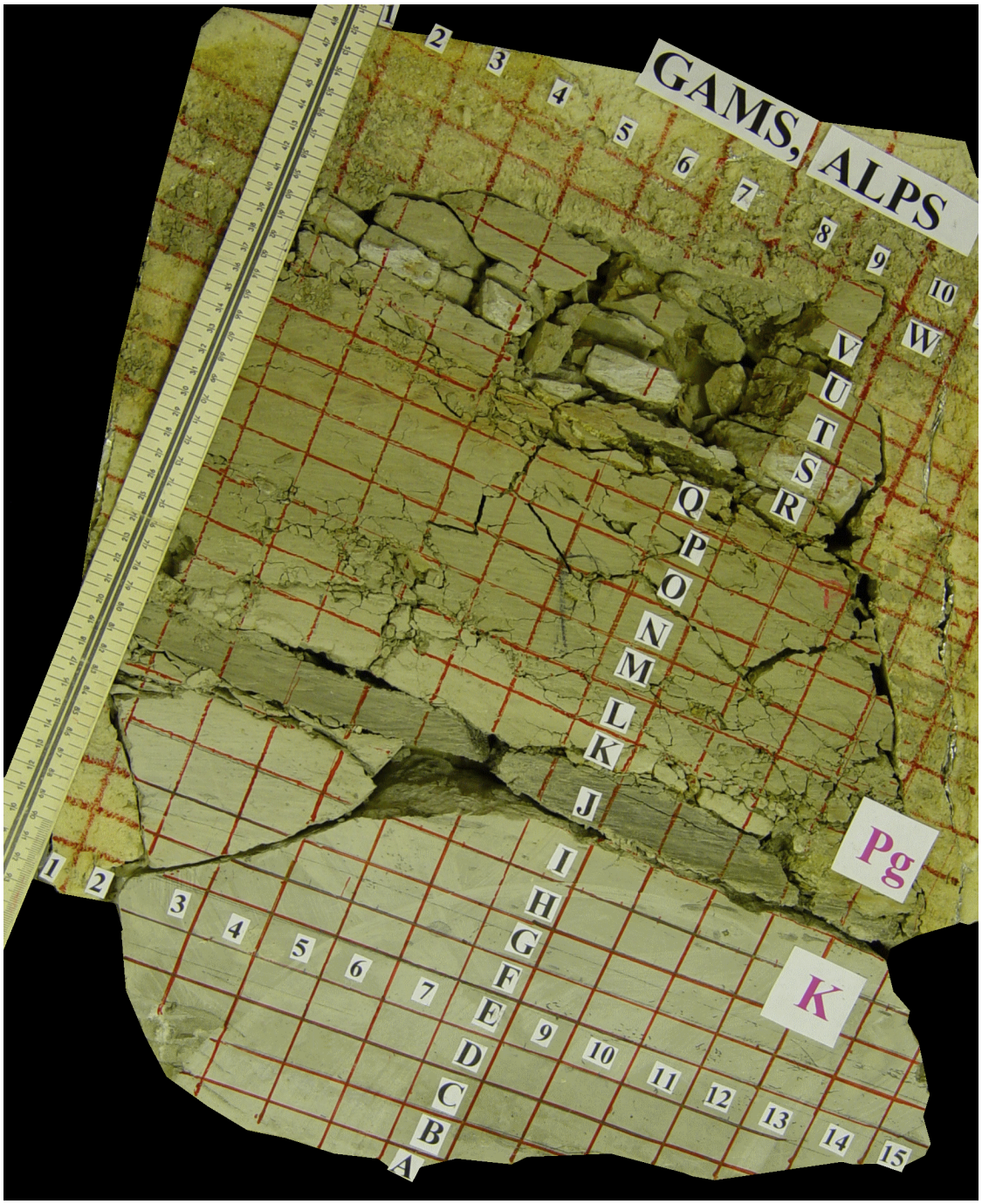

Figure 2. The Gams section monolith, prepared for sampling (photograph) [*Grachev et al.,* 2005].

istic X-ray radiation ranged from Na to U. The effective diameter of the beam was thereby close to 1–2 μm and was systematically tested at small grains. We carried out quantitative analysis of ore minerals for TiO_2, FeO, MgO, MnO, Cr_2O_3, and Al_2O_3; preliminary analysis was carried out for all elements.

[11] Selected magnetic mineral grains were prepared in compliance with a specially designed technique that ensured the ultrafine polishing of the material with the removal of its layer no thicker than 5 μm during the whole polishing process. The removed 5- to 10-μm-thick layer made it possible to expose pores in iron spherules 10–20 μm. Polishing sometimes exposed hollow metallic cosmic spherules with walls 0.5–2 μm thick. To achieve this, grains separated with the use of a powerful hand-held Nb-B-Fe magnet were placed onto a flat (polished) surface and covered with epoxy resin. The plastic was selected in such a way to ensure the minimum adhesion of epoxy resin to it. This allowed us to easily

Table 1. Chemical microprobe analyses (wt.%) of Gams chrome spinels

Element	1	2	3	4	5	6	7	8	9	10
SiO2			1.16	0.45						
Al_2O_3		10.61	11.49	9.69	11.25	8.46	9.25	8.96	7.31	10.05
Cr_2O_3	59.72	59.43	57.90	60.87	55.68	61.31	60.30	61.84	65.07	57.92
FeO	16.24	16.36	13.44	15.25	15.52	16.52	16.50	16.52	15.49	16.32
MgO	17.56	13.60	16.01	13.74	17.24	13.72	13.95	12.67	12.13	15.71
Fe^{2+}/Fe^{3+}	0.26	3.87	4.41	6.54	0.94	3.10	2.89	5.92	18.41	1.48
$Fe^{3+}/Fe^{2+}+Fe^{3+}$	0.79	0.20	0.18	0.13	0.27	0.24	0.26	0.14	0.06	0.40
Mg/Mg+Al		0.68	0.64	0.65	0.56	0.67	0.55	0.64	0.68	0.66
Cr/Cr+Al		0.78	0.77	0.81	0.77	0.83	0.81	0.82	0.86	0.79
$Mg/Mg+Fe^{2+}$	0.9	0.65	0.72	0.66	0.80	0.66	0.67	0.62	0.60	0.74

Element	11	12	13	14	15	16	17	18	19	20
Al_2O_3	8.71	7.91	9.23	9.72	9.87	9.16	8.43	10.12	6.52	2.71
Cr2O3	60.72	62.12	59.48	60.68	60.04	61.44	62.39	59.81	62.85	60.90
FeO	17.42	16.96	16.64	15.64	16.15	15.68	16.31	15.50	23.34	22.48
MgO	13.15	13.01	14.65	13.97	13.94	13.72	12.87	14.57	7.29	13.91
Fe^{2+}/Fe^{3+}	3.34	3.87	2.07	3.68	3.30	4.10	5.43	2.83	16.12	1.03
$Fe^{3+}/Fe^{2+}+Fe^{3+}$	0.23	0.20	0.32	0.27	0.23	0.20	0.16	0.26	0.06	0.49
Mg/Mg+Al	0.66	0.67	0.67	0.66	0.64	0.65	0.66	0.64	0.58	0.87
Cr/Cr+Al	0.82	0.84	0.82	0.81	0.80	0.81	0.83	0.80	0.87	0.94
$Mg/Mg+Fe^{2+}$	0.64	0.63	0.69	0.67	0.67	0.66	0.63	0.69	0.37	0.68

Note: Analyses: 1–5 – lower part, 5–12 – middle part, 13–20 – upper part of the transitional layer. Fe_2O_3 calculated from stoichimetry.

remove the sample with the examined particles after the solidification of the epoxy resin. Preparatorily to its use, the epoxy resin was degassed in vacuum to minimize the amount of bubbles in it. The sample was polished by ASM 2/1, 1/0, and 0.5/0 diamond pastes and suspension of ultrafinely dispersed diamonds on Montasupal polishing machines (on broadcloth and felt).

[12] The minerals separated in heavy liquids were mounted on a double-layer conducting carbon adhesive tape. Each specimen comprised a few hundred mineral grains ranging from fractions of a micrometer to hundreds of micrometers in size. The grains were first examined on a Camebax microprobe equipped with an optical microscope and three wave-dispersive spectrometers to rapidly locate luminescent grains (of, for example, diamond and moissanite). It was, however, hard to conduct qualitative analysis of each grain because of the very long required instrument time. Because of this, as soon as a new Tescan Vega II microprobe became available for us, we re-examined all the specimens on it. All of the identified grains were analyzed for all possible elements, from Be to Pu. The high sensitivity of the new detector made it possible to significantly decrease the electron-beam current: the analyses were carried out mostly at a current of 200 pA and 20 kV accelerating voltage. In complicated situations, the energy- and wave-dispersive spectrometers were utilized simultaneously to improve the reliability of the measurements. In the course of the re-examination of the specimens, we identified new minerals, which were often submicrometer-sized and had not been detected on the Camebax microprobe.

[13] Magnetic minerals were separated from the crushed samples by a powerful hand-held Nd-Fe-B magnet. In order to separate magnetic particles from the fine clay fraction, we applied ultrasonic pulverization in water. The operating regimes of the generator were selected in such a manner that small (no larger than a few fractions of a micrometer) magnetic particles were reliably recovered but not destroyed in the course of ultrasonic cleaning.

Overview of the Gams Stratigraphic Section

[14] The geological setting of the stratigraphic sequence near Gams (Knappengraben) was previously characterized by Kollmann (1964) and Lahodynsky (1988), who ascribed it to the Nierntal Formation (chron 29R). The portion of the sequence below the K/T boundary layer consists of alternating calcareous marlstone and marly limestone, and the portion above the boundary layer is dominated by clays with variable contents of Ca carbonate and occasional sand-silt beds. A detailed lithological-geochemical characterization of the clay boundary layer was presented in our earlier publications [*Grachev et al.,* 2005, 2007].

[15] In order to reproduce the conditions under which the K/T boundary clay layer was formed, we studied the chemistry of allogenic minerals to identify their source rocks. Inasmuch as the thickness of the boundary layer is a few centimeters and with regard for our earlier materials [*Grachev et al.,* 2005, 2007], we thoroughly examined allogenic minerals

Table 2. Chemical microprobe analyses (wt.%) of Gams Ni spinels

Element	1	2	3	4	5	6	7	8	9	10
TiO_2	–	–	–	–	–	–	–	–	–	–
Al_2O_3	1.16	1.27	0.90	10.29	4.96	1.26	11.52	7.88	9.04	5.42
Cr_2O_3	12.35	9.72	10.11	9.59	9.89	10.03	9.38	12.80	12.31	14.59
FeO	67.71	65.93	81.83	72.69	64.76	65.31	55.33	55.50	54.02	67.16
MnO	0.67	0.52	0.73	–	0.66	0.67	–	–	0.65	0.77
MgO	11.65	14.63	1.83	3.98	12.89	14.69	15.15	15.89	16.16	4.15
NiO	2.82	3.02	2.73	2.14	2.98	3.10	6.60	6.14	5.96	7.92
ZnO	3.65	4.91	1.87	1.31	3.86	4.94	1.01	1.32	1.86	
Fe^{2+}/Fe^{3+}	0.23	0.14	0.53	0.60	0.21	0.13	0.19	0.15	0.14	0.56
$Fe^{3+}/Fe^{2+}+Fe^{3+}$	0.81	0.88	0.66	0.62	0.66	0.88	0.84	0.88	0.88	0.65
Mg/Mg+Al	0.93	0.94	0.72	0.33	0.77	0.94	0.62	0.73	0.69	0.49
Cr/Cr+Al	0.88	0.84	0.88	0.38	0.57	0.84	0.35	0.54	0.48	0.28
$Mg/Mg+Fe^{2+}$	0.62	0.77	0.10	0.21	0.66	0.77	0.75	0.80	0.82	0.23

Element	11	12	13	14	15	16	17	18	19
TiO_2	–	–	0.60						
Al_2O_3	6.95	6.48	7.85	8.91	6.87	8.20	6.27	6.58	6.04
Cr_2O_3	14.11	7.03	7.04	5.94	7.87	9.01	8.98	8.62	7.88
FeO	59.17	67.59	68.39	59.96	77.02	62.11	66.09	67.33	67.45
MnO	–	–	–	–	–	1.07	0.84	1.29	1.24
MgO	11.90	11.10	9.05	20.84	1.53	13.66	11.37	10.61	10.26
NiO	7.87	7.25	7.06	7.36	6.72	3.21	3.77	3.70	3.81
ZnO	–	0.55				2.16	2.68	1.88	2.47
Fe^{2+}/Fe^{3+}	0.29	0.28	0.38	0.02	0.62	0.20	0.26	0.28	0.28
$Fe^{3+}/Fe^{2+}+Fe^{3+}$	0.77	0.78	0.73	0.98	0.62	0.83	0.79	0.78	0.78
Mg/Mg+Al	0.68	0.68	0.59	0.75	0.22	0.68	0.70	0.67	0.68
Cr/Cr+Al	0.58	0.42	0.37	0.31	0.43	0.42	0.49	0.47	0.47
$Mg/Mg+Fe^{2+}$	0.62	0.56	0.46	0.97	0.08	0.68	0.60	0.56	0.55

Note: Analyses: 1–5 – lower part, 6–12 – middle part, 13–19 – upper part of the transitional layer. Fe_2O_3 calculated from stoichimetry.

from the lower, middle, and upper portions of the sequence (A. F. Grachev et al., in press, 2008). Each of these portions was characterized by its inherent paragenetic association of minerals, which was of principal importance for our reconstructions of the conditions under which the boundary layer was produced.

[16] Because of its resistance to mechanical wearing, spinel plays a key role in reproducing the paleogeographic environment [*Lenaz et al.,* 2000; *Zhu et al.,* 2004, 2005; and others]. For the Eastern Alps, where our study area is located, the first data on the chemistry of detrital spinel in the Mesozoic sedimentary rocks, including the Upper Gosau Cretaceous-Paleogene Group, were published in [*Pober and Faupl,* 1988].

Outline of Spinel Chemistry

[17] Minerals of the spinel group were found in the Gams sequence in the K/T boundary layer of clay and in the overlying Maestrichtian clays. We determined that the rocks contain two spinel populations: Cr-spinel with a low Ni concentration (<0.1%) and spinel rich in Ni (>2%) (Tables 1, 2). The former was found throughout the whole vertical section of the Gams boundary layer, whereas the latter is contained not only in all portions of transitional layer, but also below in calcareous marlstones. The lower portion of the boundary layer commonly contains spinel in association with single grains of magnesiochromite and chromite.

[18] The two spinel populations also show different morphologies of their grains. The Cr-spinel typically occurs as angular grains with clearly pronounced serrated edges, a feature suggesting the absence of abrasion (Figure 3a). These grains range from 20 to 100–150 μm in size. The Ni-bearing spinel was found in the form of octahedral crystals up to 10–15 μm (Figure 3b,c,d).

[19] The Cr-spinel is noted for high and relatively little varying Cr_2O_3 concentrations (from 57% to 79%) and high variations in MgO (3–20%) and FeO (13–40%). Some analyses indicate the presence of TiO_2 (up to 0.6%), MnO (up to 1.6%), ZnO (up to 0.8%), V_2O_5 (up to 0.3%), and NiO (up to 0.1%) (Table 1).

[20] Spinel compositions are commonly classified on the basis of their Cr/(Cr + Al) and Mg/(Mg + Fe^{2+}) ratios. As follows from the diagram in Figure 4, spinel from the boundary layer of the Gams sequence has very high and

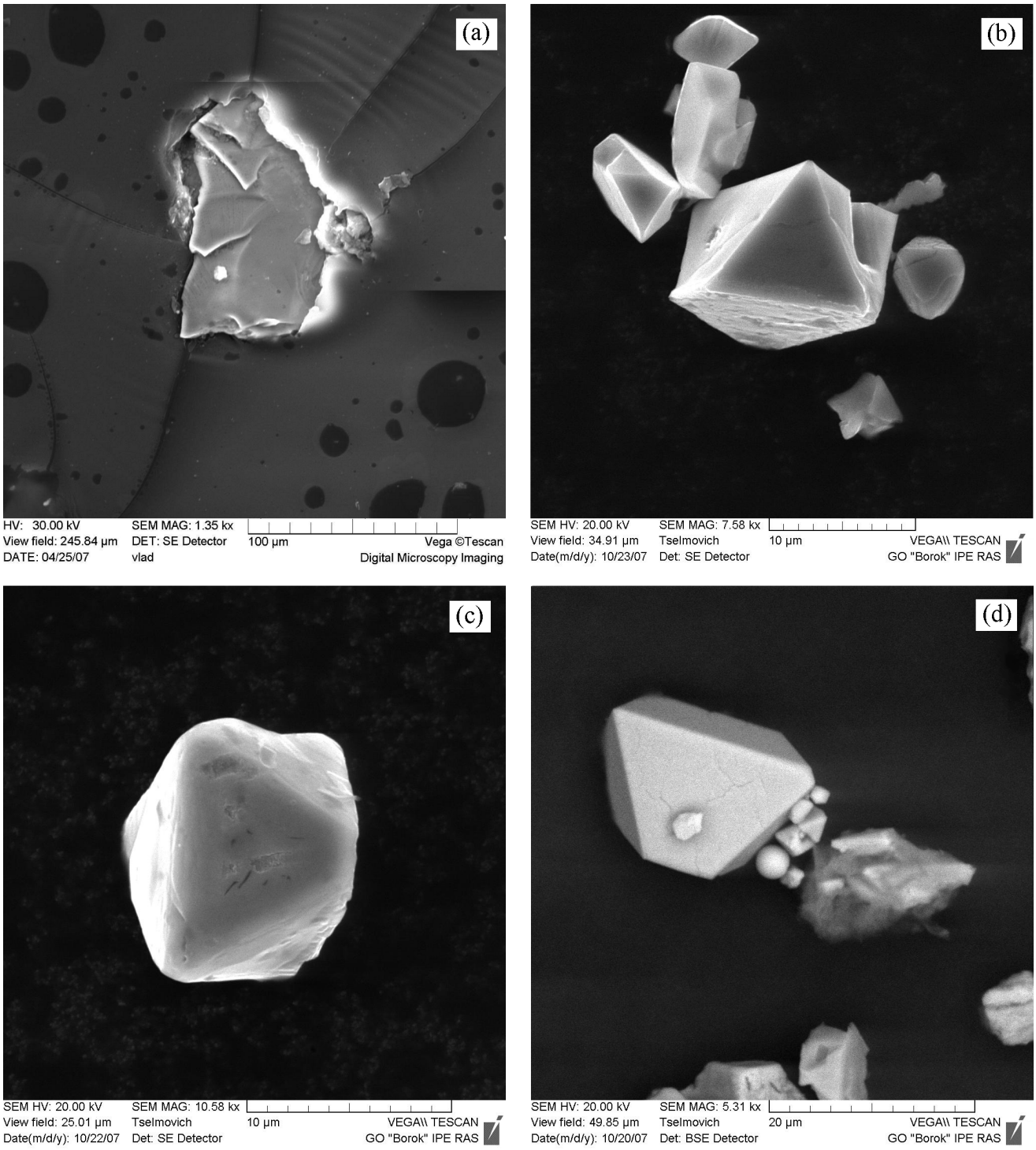

Figure 3. SEM images of spinel grains from the Gams stratigraphic sequence: a – Cr-spinel, b, c, d – Ni spinel from the lower, middle and upper parts of the transitional layer correspondingly.

little varying Cr# values ($\geq$0.8) and strongly varying Mg#.

[21] It has been demonstrated [*Pober and Faupl,* 1988] that spinel from sedimentary rocks of the Upper Gosau Group shows broad variations in its Cr# (from 0.15 to 0.85) at insignificantly varying Mg#, and its compositional points plot within the field of spinel from harzburgites and lherzolites. As can be seen in Figure 4, the compositional fields of spinel form the Gamns sequence and Gosau Group are clearly separated in the diagram, which testifies that the erosion of Alpine-type peridotites of an ophiolite association could not

provide detrital spinel for the Gams boundary layer.

[22] The origin of Cr-spinel in the clays could have been related with volcanic processes, because the influence of a mantle plume was proved for the boundary layer in the Gams sequence [*Grachev et al.,* 2005, 2007], but our samples are characterized by low TiO_2 contents (<1%). The Cretaceous Tainba Formation in southern Tibet, which has a similar age and composition, contains detrital spinel borrowed from basalts related to a mantle plume and contains up to 4% TiO_2 [*Zhu et al.,* 2004], and this mineral from Siberian and Deccan flood basalts contains 18–20% TiO_2 [*Melluso et al.,* 1995; *Zolotukhin et al.,* 1989].

[23] An appealing idea seemed to be searching for possible genetic relations between detrital spinel in the Gams sequence and chromitites in ultrabasic rocks of the Speick Complex (PR_3-PZ_1) at a distance of approximately 100 km southeast of the village of Gams [*Melcher and Meisel,* 2004]. We sampled the chromitites and examined the composition of Cr-spinel from the Kraubath Massif and used the analyses published in [*Melcher and Meisel,* 2004] for comparative analysis.

[24] The compositional fields of spinel from the Kraubath and Hochgrossen massifs, both of which belong to the Speick Complex, partly overlap the field of spinel from the Gams sequence, but their general Cr# vs. Mg# dependences are exactly opposite. Moreover, spinel from the Speick Complex is higher in TiO_2 (up to 3%) [*Melcher and Meisel,* 2004].

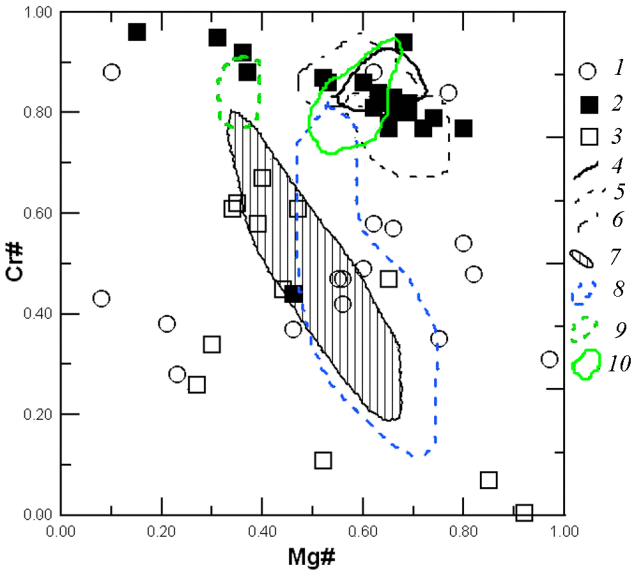

Figure 4. Cr# - Cr/(Cr+Al) - Mg# - Mg/(Mg + Fe^{2+}) diagram for spinel from the Gams stratigraphic sequence. 1 – Ni spinel, Gams sequence, 2 – same mineral from elsewhere (see Table 3), 3 – Cr-spinel, Gams sequence, 4–6 – Cr-spinel, inclusions in diamonds from South Africa and Yakutia: 4 – South Africa, 5, 6 – Yakutia [*Sobolev et al.,* 2004], 7 – Cr-spinel from the Upper Gosau Group, Eastern Alps [*Pober and Faupl,* 1988], 8 – Cr-spinel from harzburgites and lherzolites [*Stevens,* 1944], 9, 10 – Cr-spinel from chromitites, Hochgrossen and Kraubath massifs, Speick Complex, Eastern Alps [*Melcher and Meisel,* 2004].

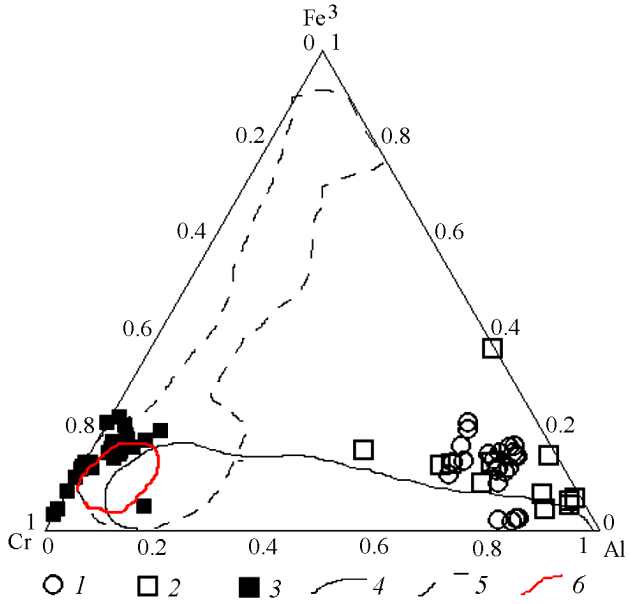

Figure 5. Cr-Fe^{3+}-Al diagram for spinel from the Gams sequence. 1 – Ni spinel from the Gams sequence, 2 – same mineral from elsewhere (see Table 3), 3 – Cr-spinel from the Gams sequence, 4 – Cr-spinel from Alpine-type ultramafic rocks [*Barnes and Roeder,* 2001], 5 – Cr-spinel from kimberlites [*Barnes and Roeder,* 2001], 6 – Cr-spinel inclusions in diamonds from kimberlites [*Sobolev,* 1974].

[25] As follows from Figures 4 and 5, the closest analogue of the Gams Cr-spinel is spinel from kimberlites and inclusions in diamonds [*Barnes and Roeder,* 2001; *Kamensky et al.,* 2002; *Sobolev,* 1974]. In a Cr# vs. Mg# diagram (Figure 4), the composition of Cr-spinel from the Gams sequence overlaps the compositions of spinel inclusions in Yakutian and South African diamonds [*Sobolev,* 1974; *Sobolev et al.,* 2004].

[26] The Cr_2O_3 vs. MgO diagram in Figure 6 accentuates this similarity revealing a common "peridotite" trend with a strong correlation between Cr and Al typical of Cr-spinel in kimberlites [*Barnes and Roeder,* 2001; *Kamensky et al.,* 2002]. The analysis of other diagrams corroborates this conclusion (Figures 7, 8, and 9).

[27] Judging from the data presented above, the detrital Cr-spinel could originate from metamorphic rocks of eclogite composition, which are widespread in Eastern Alps [*Sassi et al.,* 2004; and others]. Single spinel grains were recently found in eclogites from Pohorje [*Janak et al.,* 2006]. Diamonds were found in such rocks in many complexes throughout the world (in Kazakhstan, China, Norway, Greece, and Germany) [*Mposkos and Kostopoulos,* 2001; *Schulze et al.,* 1996; *Sobolev and Shatsky,* 1990; *Xu et al.,* 1992; and others].

[28] Ni-bearing spinel was fist found in marine deposits at the K/T boundary in Furlo and Petriccio deposits in Italy and in Hole 577 in the Pacific Ocean [*Montanari et al.,* 1983; *Smit and Kyte,* 1984] and then elsewhere, in rocks of various ages, from Archean rocks to modern cosmic dust [*Ben*

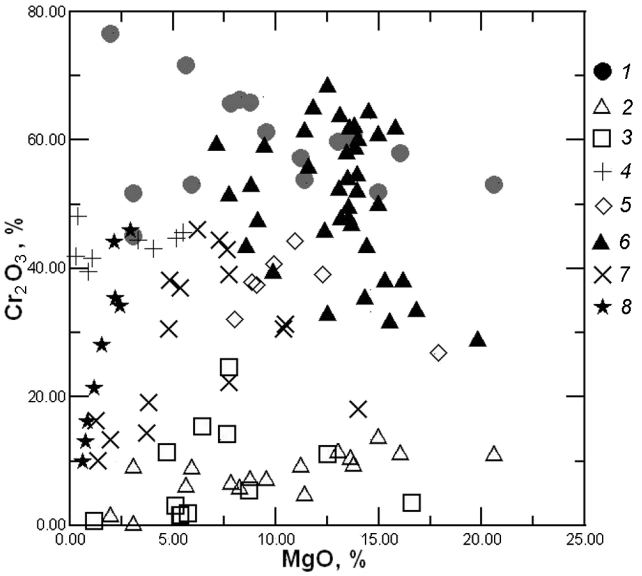

Figure 6. Cr_2O_3–MgO (wt.%) diagram for spinel from the Gams sequence in comparison with spinel from elsewhere. 1 – Cr-spinel from the Gams sequence, 2 – Ni spinel from the Gams sequence, 3 – Ni spinel from elsewhere (see Table 3), 4 – Ni spinel from the Barberton greenstone belt, 3.6 Ga, [*Byerly and Lowe,* 1994], 5 – Cr-spinel from Cretaceous flysch, Tibet [*Zhu et al.,* 2005], 6 – Cr-spinel from kimberlites [*Simandi et al.,* 2005; *Mitchel,* 1978], 7 – Cr-spinel from flood basalts [*Melluso et al.,* 1995], 8 – Cr-spinel from sulfides [*Zakrzewski,* 1989].

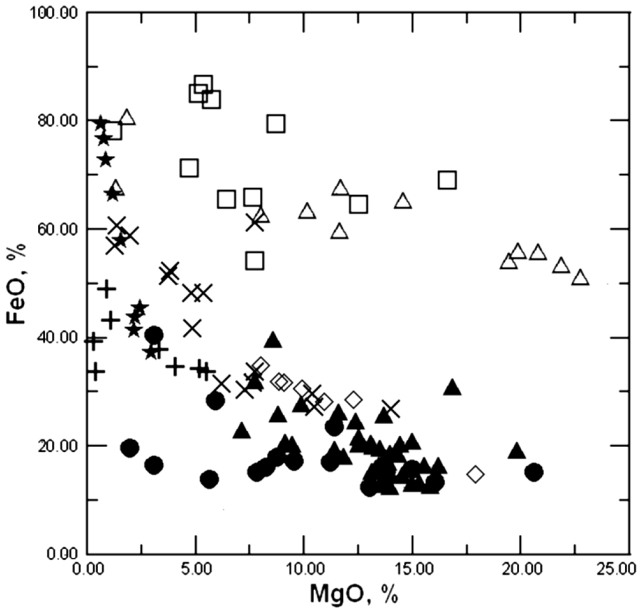

Figure 7. FeO–MgO (wt.%) diagram for spinel from the Gams sequence in comparison with spinel from elsewhere. See Figure 6 for symbol explanations.

Abdelkader et al., 1997; *Bohor et al.,* 1986; *Byerly and Lowe,* 1994; *Kyte and Bohor,* 1995; *Robin et al.,* 1992, 1991; and others]. To distinguish this spinel from spinel from magmatic rocks, the former was soon referred to as cosmic spinel [*Robin et al.,* 1992]. The typical composition of this spinel from various deposits is reported in Table 3.

[29] Since cosmic spinel was first found in rocks containing impact quartz and high Ir concentrations, the genesis of this mineral was thought to be related to the impact process [*Smit and Kyte,* 1984; and others]. However, finds of Ni spinel in rocks showing no traces of impact events, for example, in cosmic dust and micrometeorites, gave rise to an alternative viewpoint, whose proponents believed that the origin of Ni spinel was related to the ablation of a cosmic body when it entered the atmosphere [*Robin et al.,* 1992; *Toppani and Libourel,* 2003].

[30] The Gams stratigraphic sequence is principally important in the context of the genesis of Ni spinel, because spinel from these rocks contains more than 2% NiO and was detected not only in the lower part (so called rust layer) but also in the upper and middle vertical portions of the boundary layer.

[31] The chemical composition of Ni spinel from the Gams sequence is close to the composition of this mineral from elsewhere (compare Tables 2, 3). The NiO concentration

Table 3. Chemistry of Ni spinel (wt.%) from the different sections

Oxide	1	2	3	4	5	6	7	8	9	10	11
SiO_2	–	–	–	–	–	0.09	0.01	0.07	0.12	–	0.82
TiO_2	0.6	0.6	1.1	0.8	0.6	0.35	0.51	0.21	0.32	0.10	0.20
Al_2O_3	6.8	6.6	2.5	4.7	8.1	6.62	3.40	8.49	22.07	3.80	2.99
Cr_2O_3	14.2	15.5	1.9	11.5	24.7	11.16	0.65	1.03	0.20	4.70	1.61
FeO	65.9	65.5	83.9	71.4	54.2	64.64	78.28	69.10	53.97	78.90	86.85
MgO	7.6	6.4	5.7	6.7	7.7	12.52	1.15	17.96	21.02	8.60	5.34
MnO	0.7	1.0	1.3	0.8	0.7	0.27	9.94	0.40	0.58	0.10	0.17
CaO	–	–	–	–	–	0.10	0.32	0.50	0.50	–	0.03
NiO	4.2	4.4	3.6	4.1	4.0	3.67	5.50	2.29	1.41	3.80	1.64

Note: K/T boundary: 1–5 – Tunisia [*Robin et al.,* 1991]; 6 – Caravaca, Spain [*Bohor et al.,* 1986]; 7 – Furlo, Italy [*Bohor et al.,* 1986]; 8, 9 – Sites 596 and 577, Pacific [*Kyte and Bohor,* 1995]; 10 – fusion crust of Allende meteorite [*Robin et al.,* 1992]; 11 – cosmic dust [*Robin et al.,* 1991].

varies from 2% to 8%, FeO from 54% to 77%, Al_2O_3 from 1% to 10%, and Cr_2O_3 from 5% to 13%. Note that the mineral pervasively contains ZnO (up to 5%).

[32] The Cr# vs. Mg# diagram in Figure 4 shows the overlap of the compositional fields of Ni spinel from the Gams sequence and other regions, which is also illustrated in other classification diagrams (Figures 5–9). Cosmic spinel differs from terrestrial spinel in having high concentrations of Ni and Fe^{2+} and displays significant compositional variations.

[33] Another no less important identification feature is the significant difference between the $Fe^{3+}/(Fe^{2+} + Fe^{3+})$ ratios (which were calculated from stoichiometric considerations, Table 3) of magmatic and cosmic spinel. This ratio is known to be utilized as an indicator of oxygen fugacity and is important for identifying the conditions under which the melt crystallized [*Toppani and Libourel,* 2003]. As follows from Tables 1 and 3, these differences are very significant for spinel from the Gams sequence: the Ni spinel has high ratios (0.62–0.98), whereas this parameter of the Cr-spinel ranges from 0.06 and 0.48. These data are consistent with data on the composition of cosmic spinel from the fusion crusts of meteorites, in which the $Fe^{3+}/(Fe^{2+} + Fe^{3+})$ ratio varies from 0.75 to 0.90 [*Robin et al.,* 1992].

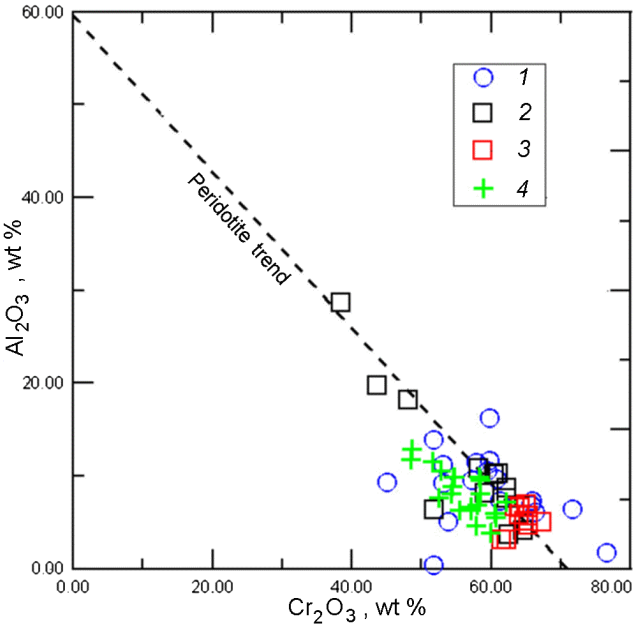

Figure 9. Cr_2O_3–Al_2O_3 (wt.%) diagram for spinel from the Gams sequence (1) in comparison with spinel from the Wawa kimberlites, Ontario, Canada (2) [*Kamensky et al.,* 2002], inclusions in diamonds (3) [*Sobolev,* 1974], PGE-Au placers of the Far East, Russia (4) [*Shcheka,* 2005].

Discussion and Conclusions

[34] Our data obtained on spinel from the K/T boundary layer in the Gams sequence, Eastern Alps, indicate that the mineral is contained in these rocks in two distinct populations. One of them is dominated by Cr-spinel that was provided for the sediments by eroded high-pressure metamorphic rocks of eclogite composition, which are widespread in the Eastern Alps. This spinel is not only typical of the whole K/T boundary layer but was also found in the overlying Maestrichtian clays. The other population of spinel principally differs from the first one in having high Ni concentrations and is contained in all parts of the boundary layer.

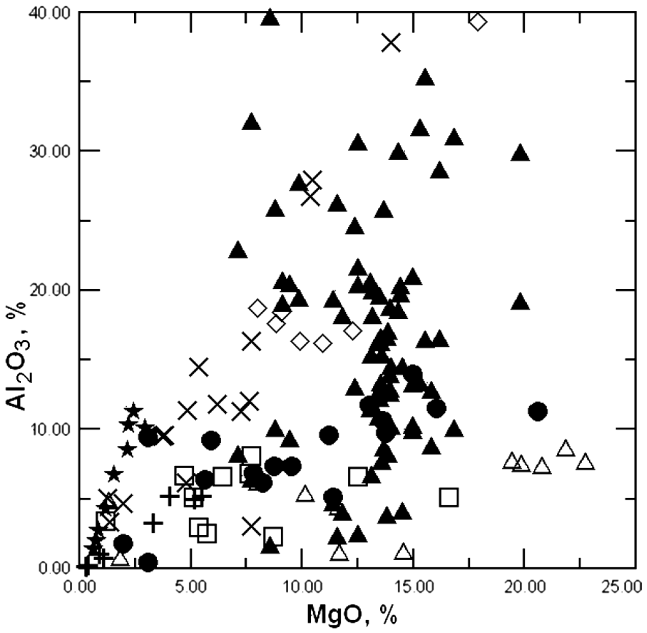

Figure 8. Al_2O_3–MgO (wt.%) diagram for spinel from the Gams sequence in comparison with spinel from elsewhere. See Figure 6 for symbol explanations.

[35] A principally important problem is the genesis of the Ni spinel, which was found, along with sediments at the Cretaceous-Paleogene boundary, also in cosmic dust, micrometeorites, cosmic spherules, and the fusion crusts of meteorites [*Toppani and Libourel,* 2003], i.e., is not directly related to any impact event.

[36] The following facts should be taken into consideration under the discussion of Ni spinel origin:

[37] 1. Ni spinel from the Gams section differs by the high content of zinc (up to 5.6% in a rust crust), that is not characteristic for other known sections at the K/T boundary.

[38] 2. Alongside with well expressed crystals octahedral forms, two grains of drop-like mode of Ni spinel has been found (Figure 7).

[39] 3. It is considered, that Ni spinel is confined to 1–3 mm rust colored layer which has deposited in less than 100 years [*Robin et al.,* 1992; etc.], while in the Gams section it meets in all parts of the transition layer.

[40] 4. Recently, in globules from the Baransky hydrothermal system (Iturup Island) have been found out such mineral phases as trevorite (Ni, Fe) Fe_2O_4, magnesiofer-

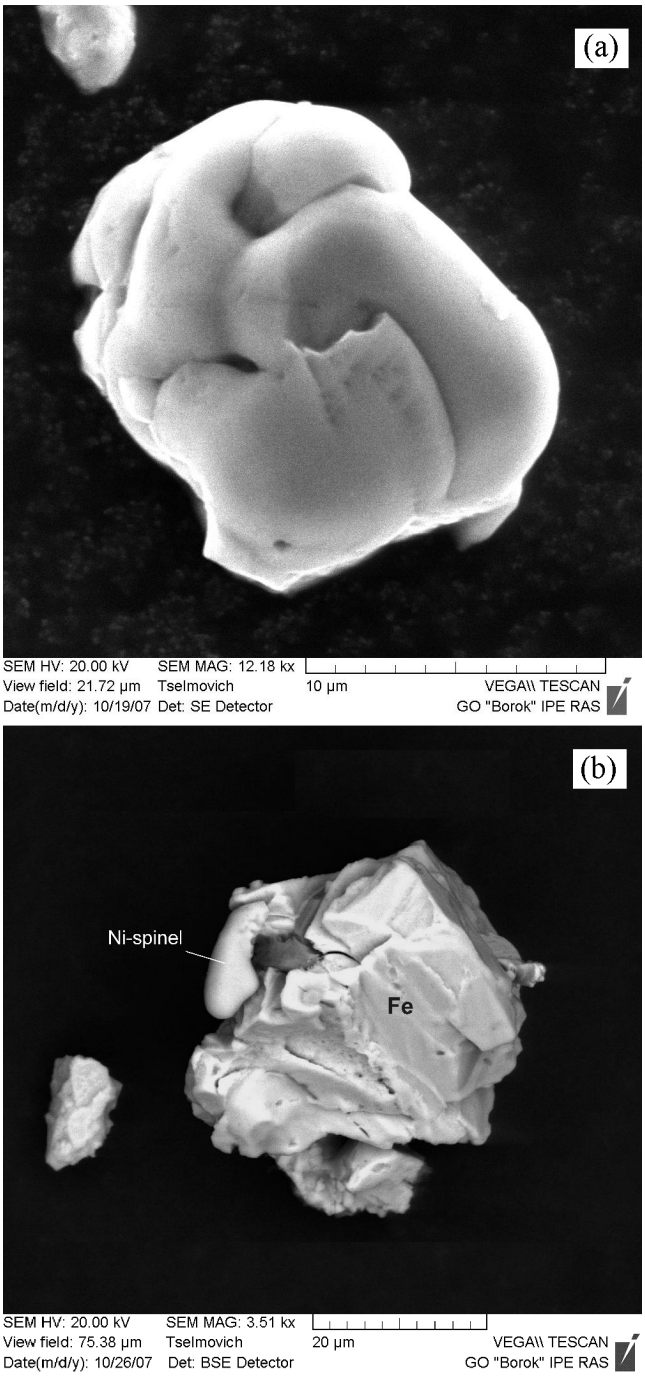

Figure 10. SEM images of the droplet Ni-spinel grains from the Gams section: a – Ni-spinel from the lower part of the transitional layer J, b – Ni-spinel extracted from the calcareous marlstones (just below Layer J, see Figure 2).

rite $MgFe_2O_4$, chromite $FeCr_2O_4$, cuprospinel CuFe2O4 together with native iron [*Rychagov et al.,* 1997]. This finding opens the another way in the study of Ni spinel formation as a result of the mantle fluid activity during the volcanic eruptions. In this connection it is necessary to note the discovery of Ni spinel in spherules from the Paleocene flood basalts in Western Greenland [*Robin et al.,* 1996]. High Cu contents in these spherules exclude their formation from meteoritic material. It is important that the enclosed basalts have the abnormal Ir concentrations (up to 6.8 ng g^{-1}) [*Robin et al.,* 1996].

[41] Thus, the question of origin Ni spinels from the transitional layer at the K/T boundary remains opened and demands the further researches.

[42] **Acknowledgments.** This work was supported by the President of the Russian Federation (the program "Leading Scientific Schools," grant no. RSh-1901.2003.5) and the RFBR grants 06-05-65162 and INTAS-03-51-5807.

References

Alvarez, L. W., W. Alvarez, F. Asaro, and H. V. Michel (1980), Extraterrestrial causes for the Cretaceous-Tertiary extinction, *Science, 208,* 1095, doi:10.1126/science.208.4448.1095.

Barnes, S. J., and P. L. Roeder (2001), The range of spinel compositions in terrestrial mafic and ultramafic rocks, *J. Petrol., 42,* 2279, doi:10.1093/petrology/42.12.2279.

Ben Abdelkader, O., H. Ben Salem, and P. Donze (1997), The K/T Stratotype section of El Kef (Tunisia): Events and biotic turnovers, *Geobios.,* 21, 235, doi:10.1016/S0016-6995(97)80098-8.

Bohor, B. F., E. E. Foord, and R. Ganapathy (1986), Magnesioferrite from the Cretaceous-Tertiary boundary, Caravaca, Spain, *Earth Planet. Sci. Lett., 81,* 57, doi:10.1016/0012-821X(86)90100-7.

Byerly, G. R., and D. R. Lowe (1994), Spinel from archean impact spherules, *Geochim. Cosmochim. Acta., 58,* 3469, doi:10.1016/0016-7037(94)90099-X.

Dolenec, T., J. Pavsic, and S. Lojen (2000), Ir anomalies and other elemental markers near the Palaeocene-Eocene boundary in a flysch sequence from the Western Tethys (Slovenia), *Terra Nova., 12,* 199, doi:10.1046/j.1365-3121.2000.00292.x.

Ellwood, B., W. MacDonald, C. Wheeler, and S. Benoist (2003), The K-T boundary in Oman: Identified using magnetic susceptibility field measurements with geochemical information, *Earth Planet. Sci. Lett., 206,* 529, doi:10.1016/ S0012-821X(02)01124-X.

Grachev, A., I. Kamensky, O. Korchagin, and H. Kollmann (2007), First data on He isotopic signatures in the Cretaceous-Paleogene clay boundary layer at Gams, Eastern Alps, *Izv. Phys. Solid Earth, 43*(9), 7.

Grachev, A. F., O. A. Korchagin, and V. A. Tselmovich (2006), Cosmic material in clay from the Cretaceous-Paleogene boundary layer at Gams, Eastern Alps, in *Physicochemical and Petrophysical Studies in Earth Sciences,* 7th Int. Conf.,, p. 21, Institute of Physics of the Earth (IPE), Moscow.

Grachev, A., O. Korchagin, H. Kollmann, D. Pechersky, and V. Tsel'movich (2005), A new look at the nature of the transitional layer at the K/T boundary near Gams, Eastern Alps, Austria and the problem of the mass extinctions of the Biota, *Russian J. Earth Sci., 7*(6), 1, doi:10.2205/2005ES000189.

Graup, G., and B. Spettel (1989), Mineralogy and phase-chemistry of an Ir-Enriched pre-K/T layer from the Lattengebirge, Bavarian Alps, and significance for the KTB problem, *Earth Planet. Sci. Lett., 95,* 271, doi:10.1016/0012-821X(89)90102-7.

Janak, M., N. Froitzheim, and M. Vravec (2006), Ultrahigh-Pressure metamorphism and exhumation of garnet peridotite in Pohorje, Eastern Alps, *J. Metamorphic. Geol., 24,* 19, doi:10.1111/j.1525-1314.2005.00619.x.

Kamensky, F. V., S. M. Sablukov, and L. I. Sablukova (2002),

Kimberlites from the Wawa Area, Ontario, *Can. J. Earth Sci., 39,* 1819, doi:10.1139/e02-089.

Keller, G., and W. Stinnesbeck (2000), Iridium and the K/T boundary at El caribe, Guatemala, *Int. J. Earth Sci., 88,* 840, doi:10.1007/s005310050310.

Kyte, F. T., and B. R. Bohor (1995), Nickel-Rich magnesiwustite in Cretaceous-Tertiary boundary spherules crystallized from ultramafic, refractory silicate liquids, *Geochim. Cosmochim. Acta, 59,* 4967, doi:10.1016/0016-7037(95)00343-6.

Lenaz, D., V. S. Kamenetsky, A. J. Crawford, and F. Princivalle (2000), Melt inclusions in detrital spinel from the SE Alps (Italy-Slovenia): A new approach to provenance studies of sedimentary basins, *Contrib. Mineral. Petrol., 139,* 748, doi:10.1007/s004100000170.

Melcher, F., and Th. Meisel (2004), A metamorphosed Early Cambrian Crust-Mantle transition in the Eastern Alps, Austria, *J. Petrol., 45,* 1689, doi:10.1093/petrology/egh030.

Melluso, L., L. Beccaluva, P. Brotzu, A. Gregnanin, A. Gupta, L. Morbidelli, and G. Traversa (1995), Constraints on the nature of the mantle sources beneath the Deccan Traps from the petrology and geochemistry of the basalts from Gujarat (Western India), *J. Petrol., 36,* 1393.

Mitchel, R. H. (1978), Mineralogy of the Elwin Bay Kimberlites, Somerset Island, N.W.T. Canada, *Am. Mineral., 63,* 47.

Montanari, A., R. L. Hay, and W. Alwarez (1983), Spheroids at the Cretaceous-Tertiary boundary are altered impact droplets of basaltic composition, *Geology, 11,* 668, doi:10.1130/0091-7613(1983)11<668:SATCBA>2.0.CO;2.

Mposkos, E. D., and D. K. Kostopoulos (2001), Diamond, former coesite and supersilicic garnet in metasedimentary rocks from the Greek Rhodope: A new ultrahigh-pressure metamorphic Province Established, *Earth Planet. Sci. Lett., 192,* 497, doi:10.1016/S0012-821X(01)00478-2.

Pober, E., and P. Faupl (1988), The chemistry of detrital chromian spinel and its implications for the geodynamic evolution of the Eastern Alps, *Geol. Rundsch., 77,* 641, doi:10.1007/BF01830175.

Robin, E., R. Rocchia, and I. Lefevre (1991), The compositional variation of K/T spinel in Tunisia: Evidence for a global deluge of projectile debris, *Earth Planet. Sci. Lett., 107,* 715.

Robin, E., Ph. Bonte, and L. Froget (1992), Formation of spinels in cosmic objects during atmospheric entry: A clue to the Cretaceous-Tertiary boundary event, *Earth Planet. Sci. Lett., 108,* 181, doi:10.1016/0012-821X(92)90021-M.

Robin, E., N. H. M. Swinburne, L. Froge, R. Rocchia, and J. Gayraud (1996), Characteristics and origin of the glass spherules from the Paleocene flood basalt province of western Greenland, *Geochim. Cosmochim. Acta., 60,* 815, doi:10.1016/0016-7037(95)00433-5.

Rychagov, S. N., S. F. Glavatskich, and E. I. Sandimirova (1997), Ore ans silicate magnetic globules as an indicators of structure and fluid regime of modern hydrothermal system of Baransky volcano, Iturup Island, *Transactions (Doklady) of the Russian Academy of Sciences, 356,* 677.

Sassi, R., C. Mazzoli, Ch. Miller, and J. Konzett (2004), Geochemistry and metamorphic evolution of the Pohorie mountain eclogites from the Austroalpine basement of the Eastern Alps (Northern Slovenia), *Lithos., 78,* 235, doi:10.1016/j.lithos.2004.05.002.

Schulze, D. I., D. Wiese, and J. Steude (1996), Abundance and distribution of diamonds in eclogites revealed by volume visualization of CT X-ray scans, *J. Geol., 104,* 109.

Shcheka, G. G. (2005), Platinum-Group mineralogy of PGE-Au placers of the Southern Far East, *Russia, Dissertation,* p. 152, Technical University, Clausthal.

Simandi, G. J., T. Ferbey, and V. M. Levson (2005), Kimberlite and diamond indicator minerals in Northeast British Columbia, Canada – A reconnaissance survey, British Columbia Ministry of Energy, Mines Petroleum Resources *Geofile, (25)* 25 pp., *Science Sections.* (in Russian), *356,* 677.

Smit, J., and F. T. Kyte (1984), Siderophile-Rich magnetic spheroids from the Cretaceous-Tertiary boundary in Umbria, *Nature, 310,* 403, doi:10.1038/310403a0.

Sobolev, N. V. (1974), *Deep Nodules in Kimberlites and the Problem of the Upper Mantle Composition,* 264 pp., Nauka, Novosibirsk.

Sobolev, N. V., and V. S. Shatsky (1990), Diamond inclusions in garnets from metamorphic rocks: A new environment for diamond formation, *Nature, 343,* 742.

Sobolev, N. V., A. M. Logvinova, and D. A. Zedgenezov (2004), Mineral inclusions in microdiamonds from kimberlites of Yakutia: A comparative study, *Lithos, 77,* 225, doi:10.1016/j.lithos.2004.04.001.

Stevens, R. E. (1944), Compositions of some chromites of the Western Hemisphere, *Am. Mineral., 29,* 1.

Toppani, A., and G. Libourel (2003), Factors controlling compositions of cosmic spinels: Application to atmospheric entry conditions of meteoritic materials, *Geochim. Cosmochim. Acta., 67,* 4621, doi:10.1016/S0016-7037(03)00383-1.

Wagreich, M., and H.-G. Krenmayr (2005), Upper Cretaceous oceanic red beds (CORB) in the Northern Calcareous Alps (Nierental Formation, Austria): slope topography and clastic input as primary controlling factors, *Cretaceous Res., 26,* 57, doi:10.1016/j.cretres.2004.11.012.

Xu, S., A. I. Okay, and A. Sengor (1992), Diamond from the dabie shan metamorphic rocks and its implications for tectonic setting, *Science, 256,* 80, doi:10.1126/science.256.5053.80.

Zakrzewski, M. (1989), Chromian spinel from Kusa, Bergslagen, Sweden, *Am. Mineral., 74,* 448.

Zhu, B., J. W. Delano, and W. S. F. Kidd (2005), Magmatic compositions and source terranes estimated from melt inclusions in detrital Cr-rich spinels: An example from mid-cretaceous sandstones in the Eastern Tethys Humalaya, *Earth Planet. Sci. Lett., 233,* 295, doi:10.1016/j.epsl.2005.02.001.

Zhu, B., W. S. F. Kidd, D. B. Rowley, and B. S. Currie (2004), Chemical compositions and tectonic significance of chrome-rich spinels in the Tianba Flysch, Southern Tibet, *J. Geol., 112,* 417.

Zolotukhin, V. V., Yu. R. Vasiliev, and O. A. Dyuzhikov (1989), *Diversity of flood basalts and their parental magmas: An example of the Siberian Platform,* 245 pp., Nauka, Novosibirsk.

A. F. Grachev, Schmidt Institute of Physics of the Earth, Russian Academy of Sciences, Moscow, Russia

H. A. Kollmann, Museum of Natural History, Vienna, Austria

O. A. Korchagin, Geological Institute, Russian Academy of Sciences, Moscow, Russia

V. A. Tselmovich, Geophysical Observatory, Schmidt Institute of Physics of the Earth, Russian Academy of Sciences, Borok, Yaroslavl oblast, Russia